AC Stark shift of the Cs microwave atomic clock transitions

P. Rosenbusch
LNE-SYRTE, Observatoire de Paris, 75014 Paris, France

S. Ghezali
Department of Physics, University Sad Dahlab, Blida, and Laboratory of Quantum Electronics, University of Sciences and Technology HOUARI BOUMEDIENE, Bab-Ezzouar, Alger, Algeria

V. A. Dzuba and V. V. Flambaum
School of Physics, University of New South Wales, Sydney, 2052, Australia

K. Beloy and A. Derevianko
Department of Physics, University of Nevada, Reno, Nevada 89557

(Dated: October 23, 2008)

We analyze the AC Stark shift of the Cs microwave atomic clock transition theoretically and experimentally. Theoretical and experimental data are in a good agreement with each other. Results indicate the absence of a magic wavelength at which there would be no differential shift of the clock states having zero projections of the total angular momentum.

PACS numbers: 06.30.Ft, 37.10.Jk, 31.15.A-

I. INTRODUCTION

The present definition of the unit of time, the second, is based on the frequency of the microwave transition between two hyperfine levels of the Cs atom. Recently, it has been realized that the accuracy and stability of atomic clocks can be substantially improved by trapping atoms in optical lattices operated at a certain "magic" wavelength [1, 2]. At this magic wavelength, both clock levels experience the same AC Stark shift; the clock frequency becomes essentially independent on trapping laser intensity.

This effect was demonstrated [3, 4, 5] for optical clocks using strontium atoms. An extension of this idea to microwave clocks with alkali-metal atoms Rb and Cs was considered in Ref. [6]. A multitude of magic wavelengths for the hyperfine transition was identified. Unfortunately, detailed analysis presented below shows the conclusions of that paper to be erroneous: there is no magic wavelength for Cs, at least for clock levels with zero projections of the total angular momentum M_F on the quantizing magnetic field. In a separate paper [7] we analyze the case of circular light polarization and $M_F \neq 0$ levels and demonstrate that the AC shift can be eliminated by an appropriate "magic angle" choice of the direction of the magnetic field with respect to the light propagation.

This paper presents a detailed theoretical analysis of the frequency shift of a microwave clock involving a hyperfine transition. The analysis requires calculation of the differential polarizability involving third-order expressions, quadratic in the field strength and linear in the hyperfine interaction. Evaluation of the resulting expressions is carried out using relativistic many-body theory. The second part of the paper reports measurements of the clock shift at two laser wavelengths. The results of the calculations are in a good agreement with the experimental measurements.

II. THEORY

Here we follow the formalism of the quasi-energy states reviewed in the context of laser-atom interaction in Ref. [8]. We start with considering the AC Stark shift $\delta E^{[2]}$ in the second order of perturbation theory (quadratic in the electric field) and then extend the formalism to the higher-order AC Stark shift $\delta E^{[2+1]}$ which takes into account the hyperfine interaction (HFI). The latter shift appears in the third order of perturbation theory and is quadratic in the field amplitude and linear in the HFI. An important part of the analysis involves the tensorial expansion of the shifts in the scalar, vector, and tensor parts.

We are interested in transitions between two hyperfine components of the same electronic states. Below we employ the conventional labeling scheme for the atomic eigenstates, $|n\,(IJ)\,FM_F\rangle$, where I is the nuclear spin, J is the electronic angular momentum, and F is the total angular momentum, $\mathbf{F} = \mathbf{J} + \mathbf{I}$. M_F is the projection of F on the quantization axis and n encompasses the remaining quantum numbers. Since the clock transitions involve the same electronic state, we will also use a shorthand notation $|F, M_F\rangle$. For example, the Cs fountain clock involves transitions between hyperfine levels $|F = 4, M_F = 0\rangle$ and $|F' = 3, M'_F = 0\rangle$ of the $6s_{1/2}$ ground electronic state.

Under the influence of the laser each clock level is perturbed. The clock frequency is modified by the difference

in the perturbed energies

$$\delta\nu^{\rm Stark}\left(\omega_L\right) \;=\; \frac{1}{h}\left[\delta E^{\rm Stark}_{n(IJ)F''M''_F}\left(\omega_L\right) - \delta E^{\rm Stark}_{n(IJ)F'M'_F}\left(\omega_L\right)\right] \qquad (1)$$

At the "magic frequency", this AC Stark clock shift would vanish.

A. Second-order dynamic response

This section introduces notation and reviews derivation and tensorial analysis of the conventional second-order dynamic Stark shift. We demonstrate that for states of total electronic angular momentum $J = 1/2$ and for $M_F = 0$ levels (or for linear polarization) the second-order AC Stark shift of the clock transition vanishes.

Consider a traveling electromagnetic wave of an arbitrary polarization,

$$\vec{\mathcal{E}} = \frac{1}{2}\mathcal{E}_L\hat{\varepsilon}\; e^{-i(\omega t - kz)} + c.c.\;,$$

with the complex polarization vector parameterized by an angle θ

$$\hat{\varepsilon} = \hat{\mathbf{e}}_x\cos\theta + i\hat{\mathbf{e}}_y\sin\theta. \qquad (2)$$

The parametric angle θ may be related to the degrees of linear, $l = \cos 2\theta$, and circular, $A = \sin 2\theta$, polarization. Notice that the quantizing axis z is chosen along the propagation vector $\hat{\mathbf{k}}$ of the laser. The field amplitude $\mathcal{E}_L$ is related to the intensity of the laser as $I_L = \frac{c}{8\pi}\mathcal{E}_L^2$, or in practical units $I_L\left[\frac{\rm mW}{\rm cm^2}\right] \approx 1.33\times\left(\mathcal{E}_L\left[\frac{\rm V}{\rm cm}\right]\right)^2$.

In the dipole approximation, the coupling can be represented as (*h.c.* is a hermitian conjugate)

$$V_{E1}\left(t\right) \equiv -\vec{\mathcal{E}}\cdot\mathbf{D} = -\frac{1}{2}\mathcal{E}_L\;\hat{\varepsilon}\cdot D e^{-i\omega t} + h.c..$$

Application of the Floquet formalism (dressed states) yields the second-order AC shift of the atomic energy level a

$$\delta E_a^{[2]} \;=\; \sum_b \frac{\left|\langle\psi_b|v|\psi_a\rangle\right|^2}{E_a - \left(E_b - \omega\right)} + \sum_b \frac{\left|\langle\psi_a|v|\psi_b\rangle\right|^2}{E_a - \left(E_b + \omega\right)},$$

where $v = -\frac{1}{2}\mathcal{E}_L\;\hat{\varepsilon}\cdot\mathbf{D}$, ψ_a and ψ_b being the stationary atomic states with unperturbed energies E_a and E_b, respectively.

Now we proceed to the conventional reduction of the polarizability into a sum over irreducible tensor operators. Introducing the resolvent operator (H_0 is the unperturbed atomic Hamiltonian)

$$R_{E_a}\left(\omega\right) = \left(E_a - \hat{H}_0 + \omega\right)^{-1},$$

we may recast the shift as an expectation value $\delta E_a^{(2)} = \left(\frac{1}{2}\mathcal{E}\right)^2\langle\psi_a|\hat{O}_{E1}\left(\omega\right)|\psi_a\rangle$, with

$$\hat{O}_{E1}\left(\omega\right) \;=\; \left(\;\hat{\varepsilon}\cdot\mathbf{D}\right)^\dagger R_{E_a}\left(\omega\right)\left(\;\hat{\varepsilon}\cdot\mathbf{D}\right) + \left(\;\hat{\varepsilon}\cdot\mathbf{D}\right)R_{E_a}\left(-\omega\right)\;\left(\hat{\varepsilon}\cdot\mathbf{D}\right)^\dagger.$$

The order of coupling of the operators may be changed

$$\hat{O}_{E1}\left(\omega\right) \;=\; \sum_{K=0,1,2}\Big[\left(-1\right)^K \times\left\{\hat{\varepsilon}^*\otimes\;\hat{\varepsilon}\right\}_K\cdot\left\{\mathbf{D}\otimes\;R_{E_a}\left(\omega\right)\mathbf{D}\right\}_K + \left\{\hat{\varepsilon}^*\otimes\;\hat{\varepsilon}\right\}_K\cdot\left\{\mathbf{D}\otimes\;R_{E_a}\left(-\omega\right)\mathbf{D}\right\}_K\Big]\;,$$

leading to the conventional decomposition into the scalar ($K = 0$), vector ($K = 1$), and tensor ($K = 2$) terms. Here we employed $\left\{\hat{\varepsilon}\otimes\;\hat{\varepsilon}^*\right\}_{KM} = \left(-1\right)^K\left\{\hat{\varepsilon}^*\otimes\;\hat{\varepsilon}\right\}_{KM}$ and the fact that $\hat{\varepsilon}$ and $\mathbf{D}$ are rank 1 tensors. The M_K component of the compound tensor of rank K composed from components of the tensors A_{K_1} and B_{K_2} (of rank K_1 and K_2) is defined as $\left\{A_{K_1}\otimes B_{K_2}\;\right\}_{KM_K} = \sum_{M_1M_2} C^{KM_K}_{K_1M_1K_2M_2}A_{K_1M_1}B_{K_2M_2}$, where $C^{KM_K}_{K_1M_1K_2M_2}$ are the Clebsch-Gordan coefficients. The generalized scalar product is defined as $\left(A_K\cdot B_K\right) = \sum_{M_K}\left(-1\right)^{M_K}A_{KM_K}B_{K,-M_K}$.

Using the Wigner-Eckart theorem, a matrix element between two atomic states may be expressed as

$$\langle FM_F|\hat{O}_{E1}\left(\omega\right)|FM'_F\rangle \;=\; \sum_{K=0,1,2}\left(-1\right)^K\sum_\mu\left(-1\right)^\mu \times\left\{\hat{\varepsilon}^*\otimes\;\hat{\varepsilon}\right\}_{K,-\mu}\left(-1\right)^{F-M_F} \times\begin{pmatrix} F & K & F\\ -M_F & \mu & M'_F\end{pmatrix}\alpha^{(K)}_{nF}\left(\omega\right),$$

with the reduced polarizabilities

$$\begin{aligned}\alpha^{(K)}_{nF}\left(\omega\right) \;&=\; \langle nF||\left\{D\otimes\;R_{E_{nF}}\left(\omega\right)D\right\}_K + \left(-1\right)^K\left\{D\otimes\;R_{E_{nF}}\left(-\omega\right)D\right\}_K||nF\rangle\\ &=\; \sqrt{[K]}(-1)^{K+2F}\sum_{F'}\begin{Bmatrix}1 & 1 & K\\ F & F & F'\end{Bmatrix} \times\sum_{n'}\langle nF||D||n'F'\rangle\langle n'\,F'||D||nF\rangle \times\left(\frac{1}{E_{nF} - E_{n'F'} + \omega} + \left(-1\right)^K\frac{1}{E_{nF} - E_{n'F'} - \omega}\right).\end{aligned} \qquad (3)$$

Here we have used the shorthand notation $[K]\equiv(2K+1)$. The matrix element may be simplified further using specific parametrization, Eq. (2), of the polarization vector. Explicitly,$\left\{\hat{\varepsilon}^*\otimes\;\hat{\varepsilon}\right\}_{00} = -\frac{1}{\sqrt{3}}$, $\left\{\hat{\varepsilon}^*\otimes\;\hat{\varepsilon}\right\}_{1\mu} = -\frac{\sin 2\theta}{\sqrt{2}}\delta_{\mu,0}$, $\left\{\hat{\varepsilon}^*\otimes\;\hat{\varepsilon}\right\}_{2\mu} = -\frac{1}{\sqrt{6}}\delta_{\mu,0} + \frac{1}{2}\cos 2\theta\;\delta_{\mu,\pm 2}$.

Finally, the AC Stark energy shift reads

$$\delta E^{(2)}_{nFM_F} = -\left(\frac{1}{2}\mathcal{E}_L\right)^2 \left[\alpha^s_{nF}(\omega) + A\,\alpha^a_{nF}(\omega)\frac{M_F}{2F} - \alpha^T_{nF}(\omega)\frac{3M_F^2 - F(F+1)}{2F(2F-1)}\right], \quad (4)$$

with the conventional scalar, vector, and tensor polarizabilities

$$\alpha^s_{nF}(\omega) = \frac{1}{\sqrt{3}}\frac{1}{\sqrt{[F]}}\alpha^{(0)}_{nF}(\omega),$$
$$\alpha^a_{nF}(\omega) = -\frac{1}{\sqrt{2}}\frac{1}{\sqrt{[F]}}\frac{2F}{\sqrt{F(F+1)}}\alpha^{(1)}_{nF}(\omega), \quad (5)$$
$$\alpha^T_{nF}(\omega) = -\frac{2}{\sqrt{6}}2F(2F-1)\left[\frac{(2F-2)!}{(2F+3)!}\right]^{1/2}\alpha^{(2)}_{nF}(\omega).$$

In general, there is an off-diagonal $M_F = M'_F \pm 2$ optical coupling involving the tensor part of the polarizability. In practice, a quantizing **B**-field is applied along the propagation of the laser wave, and as long as the off-diagonal coupling is much smaller than the Zeeman intervals, it can be disregarded.

Since the dipole matrix elements do not couple to the nuclear degrees of freedom, the dependence of the reduced polarizabilities on I and F may be be factored out as

$$\alpha^{(K)}_{nF}(\omega) = (-1)^{J+I+F+K}\,[F]\left\{\begin{array}{ccc} J & F & I \\ F & J & K\end{array}\right\}\bar{\alpha}^{(K)}_{nJ}(\omega),$$

where the quantities $\bar{\alpha}^{(K)}_{nJ}(\omega)$ are the reduced matrix elements in the $|nJM_J\rangle$ basis,

$$\bar{\alpha}^{(K)}_{nJ}(\omega) = \langle nJ||\{D\otimes R_{E_{nF}}(\omega)D\}_K + (-1)^K\{D\otimes R_{E_{nF}}(-\omega)D\}_K||nJ\rangle.$$

These quantities do not depend on either I or F.

With this factorization, we can make important comments specific to the case of $J = 1/2$ (e.g., ground state of alkali-metal atoms such as Rb and Cs). Due to the angular selection rules, the tensor contribution (expectation value of the rank 2 tensor) vanishes and the only contributions come from the scalar and vector parts. As the vector part of the energy shift is proportional to M_F, for $M_F = 0$ clock levels only the scalar contribution remains. The vector contribution also vanishes for the case of linear polarization ($A = 0$).

The next important step is to demonstrate that the scalar shift does not depend on F. In other words, there is no clock shift at the second order. Indeed, for the scalar term, $\alpha^s_{nF}(\omega) = \frac{1}{\sqrt{3}}\frac{1}{\sqrt{[F]}}\alpha^{(0)}_{nF}(\omega) = \frac{1}{\sqrt{3}}\frac{1}{\sqrt{[J]}}\bar{\alpha}^{(0)}_{nJ}(\omega)$. This result holds for an arbitrary J.

This result has a very simple explanation. As it was pointed out above, for the case of linear polarization of laser light and $J = 1/2$ we have only a scalar contribution to the polarizability. This contribution does not depend on the orientation of the quantization axis (external magnetic field). Let us consider the case when the quantization axis is directed along the laser electric field (along the linear polarization vector **e**). From the symmetry of the problem it is obvious that the electron states $|J_z = 1/2>$ and $|J_z = -1/2>$ have exactly equal quadratic shifts. The hyperfine states $|F, F_z>$ are linear combinations of these electron states multiplied by nuclear states. Since both components, $|J_z = 1/2>$ and $|J_z = -1/2>$, of any hyperfine state have the same shift, all hyperfine states have the same shifts, i.e. the differential polarizability is equal to zero. To have a non-zero differential polarizability one has to include the hyperfine interaction. Note that the inclusion of the magnetic polarizability does not change this conclusion. If the lattice laser frequency is in optical range, the magnetic polarizability contribution is suppressed by an additional factor $\mu_B^2/D^2 \sim \alpha^2 \approx (1/137)^2$ and may be neglected.

To summarize, we arrive at the conclusion that for $J = 1/2$, $M_F = 0$ clock levels (or for linear polarization) the second-order AC Stark shift is zero. Since the calculations of Ref. [6] were limited to this second-order, their conclusions are erroneous. This is also shown in the Appendix without using irreducible tensor algebra.

B. Non-trivial effect of the hyperfine interaction

In the previous section, the HFS interaction has served the role of an "observer", as it only defined the coupling scheme. In particular, we find that the $M_F = 0$ levels of the hyperfine manifold attached to the $J = 1/2$ levels are shifted identically - at that level of approximation any laser wavelength is "magic", i.e., the clock transition remains unperturbed by any laser field. The non-trivial effect arises when we take into account the dynamic (as opposed to the observer) role of the HFS interaction.

Formally, this effect appears in the third-order double perturbation theory with two laser and one HFS interactions. We build the perturbation theory in terms of combined interaction

$$V = V_{\rm hfs} + V_{E1}(t).$$

The convenience of the Floquet formalism is that we may immediately employ the conventional formula for the third-order energy correction

$$\delta E^{[2+1]}_a = \sum_{b,c\neq a}\frac{V_{ab}V_{bc}V_{ca}}{\left(E^{(0)}_b - E^{(0)}_a\right)\left(E^{(0)}_c - E^{(0)}_a\right)} - V_{aa}\sum_{b\neq a}\frac{V_{ab}V_{ba}}{\left(E^{(0)}_b - E^{(0)}_a\right)^2},$$

Here a, b, c are dressed atomic states, i.e. $|a\rangle = |\psi_a\rangle e^{in\omega t}$, with n representing the number of photons (n could be both negative and positive). The scalar product, in addition to the conventional Hilbert space operational definition includes an averaging over the period of oscillation of

the laser field. Explicitly, after the time averaging (now a, b, and c are atomic states)

$$\delta E_a^{[2+1]}(\omega) = T_a(\omega) + C_a(\omega) + B_a(\omega) + O_a(\omega),$$

$$\begin{aligned}
T_a(\omega) &= \langle a|V_{\rm hfs} R_{E_a}(0)\, v R_{E_a}(\omega)\, v^\dagger|a\rangle \\
&\quad + \langle a|V_{\rm hfs} R_{E_a}(0)\, v^\dagger R_{E_a}(-\omega)\, v|a\rangle, \\
C_a(\omega) &= \langle a|v R_{E_a}(\omega)\, V_{\rm hfs} R_{E_a}(\omega)\, v^\dagger|a\rangle \\
&\quad + \langle a|v^\dagger R_{E_a}(-\omega)\, V_{\rm hfs} R_{E_a}(-\omega)\, v|a\rangle, \\
B_a(\omega) &= [T_a(\omega)]^*, \\
O_a(\omega) &= -(V_{\rm hfs})_{aa} \Big(\langle a|v^\dagger \left(R_{E_a}(\omega)\right)^2 v|a\rangle \\
&\quad + \langle a|v \left(R_{E_a}(-\omega)\right)^2 v^\dagger|a\rangle \Big).
\end{aligned}$$

Here $T_a(\omega)$, $C_a(\omega)$, and $B_a(\omega)$ stand for top, center, and bottom position of the HFS interaction in the respective diagram. The term $O_a(\omega)$ describes the normalization term. The relevant diagrams are shown in Fig. 1.

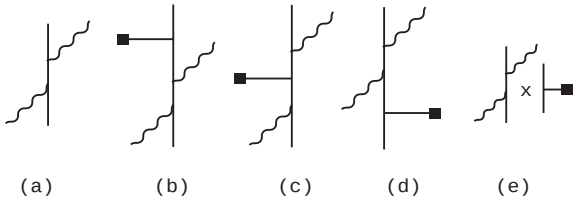

FIG. 1: Contributions to the dynamic polarizability $\alpha(\omega)$. Diagram (a) represents the second-order contribution arising from two photon interactions (wavy lines). Diagrams (b-e) represent the additional effect of the hyperfine interaction (capped line) and correspond respectively to the third-order top, center, bottom, and normalization terms as described in the text.

The interaction of the electron with the nuclear magnetic moment μ reads

$$V_{\rm hfs} = \Big(\mu \cdot \mathcal{T}^{(1)}\Big),$$

where $\mathcal{T}^{(1)}$ is the rank 1 irreducible tensor operator acting in the electronic coordinates with components

$$\mathcal{T}^{(1)}_\lambda = -\frac{|e|}{4\pi\varepsilon_0} \frac{i\sqrt{2}\left(\alpha \cdot \mathbf{C}^{(0)}_{1\lambda}(\hat{\mathbf{r}})\right)}{cr^2},$$

where α stands for the Dirac matrices and $\mathbf{C}^{(0)}_{1\lambda}(\hat{\mathbf{r}})$ are the normalized vector spherical harmonics. In the formulas below we require the reduced matrix element of the nuclear moment operator in the nuclear basis, $\langle I||\mu||I\rangle$. It is related to the nuclear magnetic g-factor as

$$\langle I||\mu||I\rangle = \frac{1}{2}\sqrt{(2I)(2I+1)(2I+2)}\, g\mu_n,$$

μ_n being the nuclear magneton.

Carrying out the angular decomposition similar to the second-order analysis of the preceding section we find that the expressions for the shift, Eq. (4), remain the same with the reduced polarizabilities $\alpha^{(K)}_{nF}(\omega)$ redefined as

$$\alpha^{(K)}_{nF}(\omega) \to \alpha^{(K)}_{nF}(\omega) + \beta^{(K)}_{nF}(\omega).$$

The third-order rank $K = 0, 1, 2$ corrections are given by the sum over contributions from diagrams of Fig. 1.

$$\beta^{(K)}_{nF}(\omega) = 2\beta^{(K)}_{nF}(\omega;\mathrm{T}) + \beta^{(K)}_{nF}(\omega;\mathrm{C}) + \beta^{(K)}_{nF}(\omega;\mathrm{O}).$$

Explicitly,

$$\beta^{(K)}_{nF}(\omega;\mathrm{T}) = [F]\sqrt{[K]} \sum_{J_a J_b} (-1)^{J+J_a} \left\{ \begin{array}{ccc} I & I & 1 \\ J_a & J & F \end{array} \right\} \left\{ \begin{array}{ccc} J & 1 & J_b \\ 1 & J_a & K \end{array} \right\} \left\{ \begin{array}{ccc} K & J & J_a \\ I & F & F \end{array} \right\} T^{(K)}_{J_a J_b}(nJ,\omega),$$

$$\beta^{(K)}_{nF}(\omega;\mathrm{C}) = [F]\sqrt{[K]} \sum_{J_a J_b} \sum_{J_i} [J_i](-1)^{2J_a+J_b+J} \left\{ \begin{array}{ccc} J & J & J_i \\ I & I & 1 \\ F & F & K \end{array} \right\} \left\{ \begin{array}{ccc} J & J & J_i \\ J_a & J_b & 1 \\ 1 & 1 & K \end{array} \right\} C^{(K)}_{J_a J_b}(nJ,\omega),$$

$$\beta^{(K)}_{nF}(\omega;\mathrm{O}) = (-1)^{2J+1}[F]\sqrt{[K]} \left\{ \begin{array}{ccc} 1 & I & I \\ F & J & J \end{array} \right\} \left\{ \begin{array}{ccc} J & J & K \\ F & F & I \end{array} \right\} \sum_{J_a} \left\{ \begin{array}{ccc} K & J & J \\ J_a & 1 & 1 \end{array} \right\} O^{(K)}_{J_a}(nJ,\omega).$$

Here we introduced the reduced sums

$$\begin{aligned}
T^{(K)}_{J_a J_b}(nJ,\omega) &= \langle I||\mu||I\rangle \sum_{n_b} \sum_{n_a \neq n} \langle nJ||\mathcal{T}^{(1)}||n_a J_a\rangle \langle n_a J_a||D||n_b J_b\rangle \langle n_b J_b||D||nJ\rangle \\
&\quad \times \left(\frac{1}{E - E_a} \frac{1}{E - E_b + \omega} + (-1)^K (\omega \to -\omega) \right),
\end{aligned} \tag{6}$$

$$C^{(K)}_{J_a J_b}(nJ,\omega) = \langle I||\mu||I\rangle \sum_{n_a n_b} \langle nJ||D||n_a J_a\rangle\langle n_a J_a||\mathcal{T}^{(1)}||n_b J_b\rangle\langle n_b J_b||D||nJ\rangle \times \left(\frac{1}{E-E_a+\omega}\frac{1}{E-E_b+\omega} + (-1)^K(\omega\to-\omega)\right), \quad (7)$$

$$O^{(K)}_{J_a}(nJ,\omega) = \langle I||\mu||I\rangle\langle nJ||\mathcal{T}^{(1)}||nJ\rangle \sum_{n_a}\langle nJ||D||n_a J_a\rangle\langle n_a J_a||D||nJ\rangle \left(\frac{1}{(E-E_a+\omega)^2} + (-1)^K(\omega\to-\omega)\right). \quad (8)$$

Notice that the angular momenta of the intermediate states J_a and J_b are fixed.

C. Numerical evaluation

To perform the calculations we use an *ab initio* approach which has been described in detail in Ref. [9]. In this approach high accuracy is attained by including important many-body and relativistic effects.

Calculations start from the relativistic Hartree-Fock (RHF) method in the V^{N-1} approximation. This means that the initial RHF procedure is done for a closed-shell atomic core with the valence electron removed. After that, the states of the external electron are calculated in the field of the frozen core. Correlations are included by means of the correlation potential method [10]. We use the all-order correlation potential $\hat{\Sigma}$ which includes two classes of the higher-order terms: screening of the Coulomb interaction and hole-particle interaction (see, e.g., [11] for details).

To calculate $\hat{\Sigma}$ we need a complete set of single-electron orbitals. We use the B-spline technique [12] to construct the basis. The orbitals are built as linear combinations of 40 B-splines of order 9 in a cavity of radius $40a_B$. The coefficients are chosen from the condition that the orbitals are the eigenstates of the RHF Hamiltonian $\hat{H}_0$ of the closed-shell core. The $\hat{\Sigma}$ operator is calculated with the technique which combines solving equations for the Green functions (for the direct diagram) with the summation over complete set of states (exchange diagram) [11].

The correlation potential $\hat{\Sigma}$ is then used to build a new set of single-electron states, the so-called Brueckner orbitals. This set is to be used in the summation in equations (6), (7), and (8). Here again we use the B-spline technique to build the basis. The procedure is very similar to the construction of the RHF B-spline basis. The only difference is that the new orbitals are now the eigenstates of the $\hat{H}_0+\hat{\Sigma}$ Hamiltonian.

Brueckner orbitals which correspond to the lowest valence states are good approximations to the real physical states. Their quality can be tested by comparing experimental and theoretical energies. Moreover, their quality can be further improved by rescaling the correlation potential $\hat{\Sigma}$ to fit the experimental energies exactly. We do this by replacing the $\hat{H}_0+\hat{\Sigma}$ Hamiltonian with $\hat{H}_0+\lambda\hat{\Sigma}$, in which the rescaling parameter λ is chosen for each partial wave to fit the energy of the first valence state. The values of λ are $\lambda_s = 1$, $\lambda_p = 0.97$, and $\lambda_d = 0.95$. Note that these values are very close to unity. This means that even without rescaling the accuracy is good and only a small adjustment of $\hat{\Sigma}$ is needed. Note also that since the rescaling procedure affects not only energies but also the wave functions, it usually leads to improved values of the matrix elements of external fields. In fact, this is a semi-empirical method to include omitted higher-order correlation corrections.

Matrix elements of the HFS and electric dipole operators are found by means of the time-dependent Hartree-Fock (TDHF) method [10, 13]. This method is equivalent to the well-known random-phase approximation (RPA). In the TDHF method, the single-electron wave functions are presented in the form $\psi = \psi_0 + \delta\psi$, where ψ_0 is the unperturbed wave function. It is an eigenstate of the RHF Hamiltonian $\hat{H}_0$: $(\hat{H}_0-\epsilon_0)\psi_0 = 0$. $\delta\psi$ is the correction due to an external field. It can be found by solving the TDHF equation

$$(\hat{H}_0-\epsilon_0)\delta\psi = -\delta\epsilon\psi_0 - \hat{F}\psi_0 - \delta\hat{V}^{N-1}\psi_0, \quad (9)$$

where $\delta\epsilon$ is the correction to the energy due to the external field ($\delta\epsilon \equiv 0$ for the electric dipole operator), $\hat{F}$ is the operator of the external field ($V_{\rm hfs}$ or $-\mathbf{D}\cdot\mathcal{E}$), and $\delta\hat{V}^{N-1}$ is the correction to the self-consistent potential of the core due to the external field.

The TDHF equations are solved self-consistently for all states in the core. Then the matrix elements between any (core or valence) states n and m are given by

$$\langle\psi_n|\hat{F}+\delta\hat{V}^{N-1}|\psi_m\rangle. \quad (10)$$

The best results are achieved when ψ_n and ψ_m are the Brueckner orbitals computed with rescaled correlation potential $\lambda\hat{\Sigma}$.

We use equation (10) for all HFS and electric dipole matrix elements in evaluating the top, center, bottom, and normalization diagrams (Eqs. (6),(7),(8)), except for the ground state HFS matrix element in the normalization diagram where we use experimental data. The results are presented in section IV.

III. EXPERIMENT

We measure the frequency shift of the Cs clock transition ($|F = 3, M_F = 0\rangle$ to $|F = 4, M_F = 0\rangle$) induced by a far detuned laser beam. A Cs fountain clock [14] is used. At each cycle $\sim 10^6$ atoms are loaded in an optical molasses and cooled to below $2\,\mu$K. Moving molasses launches the atoms upwards with a speed of 4.1 m/s where they pass twice through a microwave cavity thereby realizing Ramsey spectroscopy. The Zeeman degeneracy is lifted by a 1.6 mG magnetic field aligned along the fountains axis. The detuned laser beam is a traveling wave beam also aligned on the axis of the fountain. The light polarization is linear with respect to the light propagation. The beam waist is larger than the 11 mm diameter opening in the microwave cavity. This assures that all atoms passing through the opening and being detected experience the light. The light intensity averaged over 1 cm^2 is measured by a commercial powermeter (Newport 840-C) before entering the fountains vacuum chamber. One intensity measurement is taken before and one after each one-day run. The intensity drift between the two is of the order of 1%, however the error of the light intensity experienced by each atom is rather high. This is due to our ignorance of the exact intensity distribution, the exact atom distribution and intensity losses in the vacuum window as well as parasite reflections inside the vacuum chamber. We estimate the intensity error as 20%.

The frequency shift is measured by alternating the fountain's configuration every 50 cycles. The first configuration is the standard clock operation. The second configuration is identical to the first plus the laser beam opened during the Ramsey period. This assures that the atom preparation and cooling is not disturbed by the laser and that the atomic cloud is identical in the two configurations. Hence, we can assume that all other clock shifts, in particular collisions, are identical for the two configurations. The absolute frequency is measured for each configuration against a highly stable local oscillator exhibiting no significant drift during several hundred cycles. The frequency shift induced by the light calculates as the simple difference

$$\delta\nu = \nu_{\text{with light}} - \nu_{\text{without light}}.$$

The frequency shift is measured for a number of laser intensities. Two sets of measurements are taken for light at wavelengths of 532 nm and 780 nm. The averages of each set weighted by the statistical frequency uncertainty give a light shift of $(-3.51 \pm 0.7) \times 10^{-4}$ Hz(W/cm^2)$^{-1}$ for 532 nm and $(-2.27 \pm 0.4) \times 10^{-2}$ Hz(W/cm^2)$^{-1}$ for 780 nm. The statistical uncertainty is negligible before the uncertainty on the light intensity.

IV. RESULTS AND DISCUSSION

The shift of the clock frequency is given by (cf. Eq. (1))

$$\delta\nu_L^{\text{Stark}} = -\left(\frac{1}{2}\mathcal{E}_L\right)^2 \delta\alpha\left(\omega_L\right),$$

where $\delta\alpha\left(\omega_L\right)$ is the differential polarizability. The conversion factor between differential polarizability in atomic units and the ratio of the shift to laser intensity in practical units is given by

$$\frac{\delta\nu_L^{\text{Stark}}\,[\text{Hz}]}{I_L\left[\frac{\text{mW}}{\text{cm}^2}\right]} = -4.68 \times 10^{-5} \;\times\; \delta\alpha\left(\omega\right)[\text{a.u.}]\ .$$

We start by considering DC polarizabilities. In the static regime ($\omega_L = 0$), our calculations give $\delta\alpha = 1.82 \times 10^{-2}$ a.u., which translates into the commonly used DC Stark coefficient $k_S = -2.26 \times 10^{-10}\,\text{Hz}/(\text{V/m})^2$. Notice that this value includes only the scalar part of the polarizability. This is in agreement with the most accurate experimental result [15] of $k_S = -2.271(4) \times 10^{-10}\,\text{Hz}/(\text{V/m})^2$.

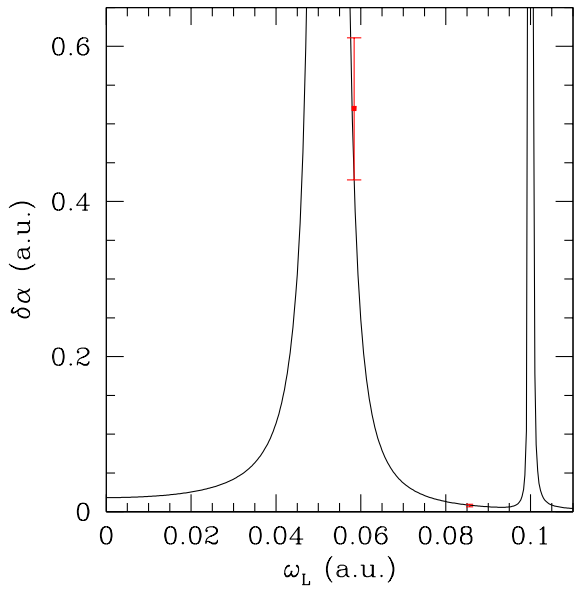

FIG. 2: (Color online) Differential polarizability of the Cs clock transition ($M_F = M_F' = 0$) in the $\mathbf{B} \parallel \hat{\mathbf{k}}$ configuration as a function of the probe laser frequency. Two experimental measurements (at 780 nm and 532 nm) are compared with theoretical predictions (solid curve). Refer to Fig. 3 for better graphical resolution of the 532 nm experimental point.

For the AC case, our calculated differential polarizability $\delta\alpha(\omega_L)$ for the cesium clock transition is presented in Fig. 2 as a function of laser frequency. Both values are given in atomic units. The two peaks correspond to the $6s - 6p$ and $6s - 7p$ resonances. The graph never crosses zero, which implies no magic frequency. Experimental

results for two laser wavelengths are also shown (also see Fig. 3). Calculated and experimental relative frequency shifts are compared in Table I and found to be in agreement with each other.

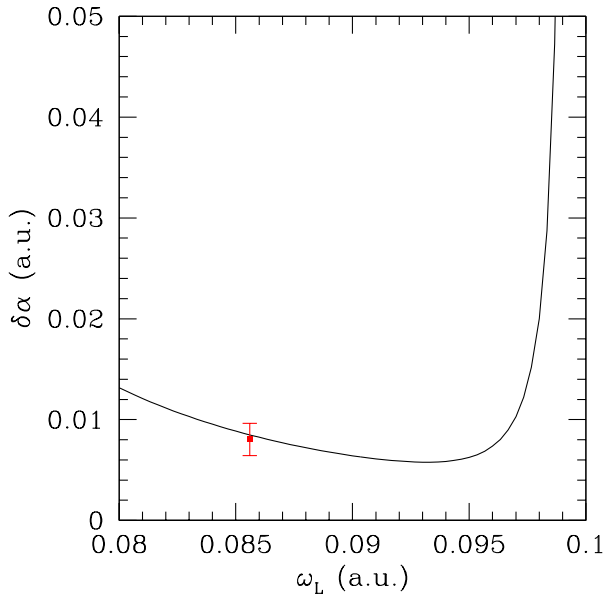

FIG. 3: (Color online) Same as in Fig. 2, in the region of the experimental point at 532 nm.

TABLE I: Comparison of the theoretical and experimental AC frequency shifts for the clock transition in Cs

λ,[nm]	ω,[a.u.]	$\delta\nu_L/I_L$, [Hz/mW/cm^2]	
		Theor.	Expt.
780	0.0584	-1.95×10^{-2}	$-2.27(40)\times10^{-2}$
532	0.0856	-3.73×10^{-4}	$-3.51(70)\times10^{-4}$

To summarize, we presented a comprehensive analysis of the AC Stark shift of the Cs microwave atomic clock transition. Theoretical analysis based on the second and third order perturbation theory is accompanied by measurements. Calculations and measurements are in good agreement with each other and indicate the absence of a magic frequency at least for the $M_F = 0$ clock levels with zero projections of the total angular momentum on the quantizing magnetic field.

APPENDIX

Considering the complexities of working with the angular algebra, here we analyze Eq. (2) of Ref. [6] for the 2nd-order dynamic Stark shift. Starting from their equation we again show that there is no AC Stark shift of the clock transition frequency. Eq. (2) of Ref. [6] for the polarizability contains a summation over M', which we manipulate

$$\sum_{M'}\begin{pmatrix} F' & 1 & F \\ M' & p & -M\end{pmatrix}^2 = (-1)^{F'-M+p}\sum_{M'}\begin{pmatrix} F & 1 & F' \\ M & -p & -M'\end{pmatrix}\begin{pmatrix} F' & 1 & F \\ M' & p & -M\end{pmatrix}$$

$$= (-1)^{F'-M+p}(-1)^{2F}\sum_{KQ}(-1)^{K-Q}[K]\begin{pmatrix} F & F & K \\ M & -M & -Q\end{pmatrix}\begin{pmatrix} K & 1 & 1 \\ Q & p & -p\end{pmatrix}\begin{Bmatrix} 1 & 1 & K \\ F & F & F'\end{Bmatrix} \quad (A.1)$$

$$= (-1)^{F-M+p}\sum_{K}(-1)^{F+F'+K}[K]\begin{pmatrix} F & K & F \\ -M & 0 & M\end{pmatrix}\begin{pmatrix} 1 & K & 1 \\ -p & 0 & p\end{pmatrix}\begin{Bmatrix} 1 & 1 & K \\ F & F & F'\end{Bmatrix}. \quad (A.2)$$

The expression (A.1) is obtained from using the summation rule 12.1(5) of Ref. [16]; we further obtain expression (A.2) by noting that only $Q = 0$ terms are non-zero in the summation.

Now we take the F'-dependent part of (A.2) with the F'-dependent part of Eq. (2) of Ref. [6] and take the summation over F'

$$\sum_{F'}(-1)^{F+F'+K}[F']\begin{Bmatrix} J & J' & 1 \\ F' & F & I\end{Bmatrix}^2\begin{Bmatrix} 1 & 1 & K \\ F & F & F'\end{Bmatrix} = \sum_{F'}(-1)^{F+F'+K}[F']\begin{Bmatrix} 1 & F & F' \\ I & J' & J\end{Bmatrix}\begin{Bmatrix} I & J' & F' \\ 1 & F & J\end{Bmatrix}\begin{Bmatrix} 1 & F & F' \\ F & 1 & K\end{Bmatrix}$$

$$= (-1)^{I-J'+F}\begin{Bmatrix} J & J & K \\ 1 & 1 & J'\end{Bmatrix}\begin{Bmatrix} J & J & K \\ F & F & I\end{Bmatrix}. \quad (A.3)$$

The expression (A.3) is obtained from using the summation rule 9.8(6) of Ref. [16].

Combining the above results gives

$$\sum_{F'M'}[F][F']\begin{pmatrix} F' & 1 & F \\ M' & p & -M\end{pmatrix}^2\begin{Bmatrix} J & J' & 1 \\ F' & F & I\end{Bmatrix}^2 = (-1)^{F-M+p}(-1)^{I-J'+F}[F]\sum_{K}[K]\begin{pmatrix} F & K & F \\ -M & 0 & M\end{pmatrix}\begin{pmatrix} 1 & K & 1 \\ -p & 0 & p\end{pmatrix}$$
$$\times\begin{Bmatrix} J & J & K \\ 1 & 1 & J'\end{Bmatrix}\begin{Bmatrix} J & J & K \\ F & F & I\end{Bmatrix}.$$

Not surprisingly, the six-j symbols here are identical to the ones appearing in the previously derived polarizabilities $\alpha_{nF}^{(K)}(\omega)$. Hence, this makes the connection to scalar ($K = 0$), vector ($K = 1$), and tensor ($K = 2$) parts.

First we focus on the case $p = 0$; this corresponds to linear polarization in the $\mathbf{B} \parallel \hat{\varepsilon}$ geometry. For $J = 1/2$ atomic states the tensor part ($K = 2$) is necessarily zero due to selection rules in the six-j symbols (this is the case regardless of polarization). Furthermore the vector part ($K = 1$) is zero due to the fact that the top row of the second three-j symbol sums to an odd number (or see (A.4) below, with $p = 0$). This leaves us with only the scalar part ($K = 0$) to analyze. In this case, the r.h.s. simply reduces to $1/(3[J]) = 1/6$. Thus we can conclude that for linear polarization of this geometry, the 2nd-order dynamic Stark shift is F-independent for $J = 1/2$ atomic states.

For the $\mathbf{B} \parallel \hat{\mathbf{k}}$ geometry, the linear polarization is regarded as an equal mixture of σ^+ ($p = +1$) and σ^- ($p = -1$) circularly polarized light. Again the tensor part is necessarily zero for $J = 1/2$. For the vector part, we note the three-j symbol relation

$$\begin{pmatrix} 1 & K & 1 \\ -p & 0 & p \end{pmatrix} = (-1)^K \begin{pmatrix} 1 & K & 1 \\ p & 0 & -p \end{pmatrix}. \qquad \text{(A.4)}$$

Thus, when we take equal mixtures of σ^+ and σ^- light, the vector contribution drops out. Again, we are left with only the scalar part. Not surprisingly, we again obtain the result $1/(3[J]) = 1/6$ when taking equal mixtures of σ^+ and σ^- light.

The above results then generalize to any geometry for linearly polarized light.

ACKNOWLEDGMENTS

This work was supported in part by the US National Science Foundation, by the Australian Research Council and by the US National Aeronautics and Space Administration under Grant/Cooperative Agreement No. NNX07AT65A issued by the Nevada NASA EPSCoR program. The SYRTE is Unité de Recherche of the Observatoire de Paris and the Université Pierre et Marie Curie associated to the CNRS (UMR8630). It is a national metrology laboratory of the Laboratoire National de Métrologie et d'Essais (LNE) and member of the Institut francilien de recherche sur les atomes froids (IFRAF). S.G. acknowledges travel support from the LNE.

[1] H. Katori, M. Takamoto, V. G. Pal'chikov, and V. D. Ovsiannikov, Phys. Rev. Lett. **91**, 173005 (2003).
[2] J. Ye, H. J. Kimble, and H. Katori, Science **320**, 1734 (2008).
[3] M. Takamoto, F. L. Hong, R. Higashi, and H. Katori, Nature (London) **435**, 321 (2005).
[4] R. Le Targat, X. Baillard, M. Fouché, A. Brusch, O. Tcherbakoff, G. D. Rovera, and P. Lemonde, Phys. Rev. Lett. **97**, 130801 (2006).
[5] A. D. Ludlow, T. Zelevinsky, and G. K. Campbell *et al.*, Science **319**, 1805 (2008).
[6] X. Zhou, X. Chen, and J. Chen (2005), arXiv:0512244.
[7] V. V. Flambaum, V. A. Dzuba, and A. Derevianko (2008), arXiv:0809.2825.
[8] N. L. Manakov, V. D. Ovsiannikov, and L. P. Rapoport, Phys. Rep. **141**, 319 (1986).
[9] E. J. Angstmann, V. A. Dzuba, and V. V. Flambaum (2006), arXiv.org:physics/0605163.
[10] V. A. Dzuba, V. V. Flambaum, P. G. Silvestrov, and O. P. Sushkov, J. Phys. B **20**, 1399 (1987).
[11] V. A. Dzuba, V. V. Flambaum, and O. P. Sushkov, Phys. Lett. A **141**, 147 (1989).
[12] W. R. Johnson, S. A. Blundell, and J. Sapirstein, Phys. Rev. A **37**, 307 (1988).
[13] V. A. Dzuba, V. V. Flambaum, and O. P. Sushkov, J. Phys. B **17**, 1953 (1984).
[14] S. Bize, P. Laurent, M. Abgrall, H. Marion, I. Maksimovic, L. Cacciapuoti, J. Grnert, C. Vian, F. P. dos Santos, P. Rosenbusch, et al., J. Phys. B **38**, S449 (2005).
[15] E. Simon, P. Laurent, and A. Clairon, Phys. Rev. A **57**, 436-39 (1998).
[16] D. A. Varshalovich, A. N. Moskalev, and V. K. Khersonskii, *Quantum Theory of Angular Momentum* (World Scientific, Singapore, 1988).